



Landscape- and climate change-induced hydrological alterations in the typically urbanized Beiyun River basin, Beijing, China

Yueqiu Zhang^{1,2} · Shiliang Liu¹ · Xiaoyun Hou¹ · Fangyan Cheng¹ · Zhenyao Shen¹

Published online: 7 November 2018

© Springer-Verlag GmbH Germany, part of Springer Nature 2018

Abstract

Landscapes in urbanized regions have experienced considerable changes in recent decades, and had a growing number of negative effects on hydrological processes. However, it is not well understood to what extent the combined and individual landscape and climate factors have altered hydrological processes in such areas. Using Beiyun River in Beijing as a case, we assessed hydrological responses quantitatively based on the Water and Energy Transfer between Soil, Plants and Atmosphere model (WetSpa extension). The results indicated that landscape patterns varied greatly from 2000 to 2012, which was exhibited primarily by the encroachment of built-up land on cropland. The landscape indices selected showed that the landscapes are prone to be disaggregated, fragmented, and complicated due to urbanization. In addition, the WetSpa model is available to simulate daily hydrological processes after calibration with model bias, model confidence and Nash–Sutcliffe efficiency of 18%, 0.71 and 0.84, respectively, and validation with correlation coefficient of 0.81. The model output revealed that the combined effects of landscape pattern change and climate variations increased total runoff and daily active groundwater storage. Among different sub-catchments, the Shahe sub-catchment upstream and Feng-gangjianhe sub-catchment downstream had higher discharges, with increasing trends from 2000 to 2012. Compared with period 1 (2000–2005) as the reference, the annual average runoff during period 2 (2006–2011) and period 3 (2012–2016) increased 16.5 mm and 77.5 mm and the daily groundwater storage increased 71.6 mm and 47.3 mm through the combined effects of landscape and climate change. In period 2, the individual climate change had a positive effect on runoff with the contribution rate of 120.6% while landscape variation had a negative effect with the rate of – 20.6%. In period 3, they both had positive effects on runoff with the contribution rates of 93.6% and 6.4%, respectively. This study has practical significance for evaluation of the influence of urbanization on the hydrological processes and future water resource management.

Keywords Landscape pattern · Climate change · Hydrological process · WetSpa extension · Beiyun River

Abbreviations

PD	Patch density
LPI	Largest Patch Index
AI	Aggregation Index
SPLIT	Splitting Index
SHAPE-AM	Area Weighted Shape Index
ED	Edge density

COHESION	Patch Cohesion Index
SHDI	Shannon's Diversity Index
<i>Ens</i>	Nash–Sutcliffe efficiency
R_e	Relative error
R	Correlation coefficient
Q_s	Surface runoff
Q_i	Interflow
Q_g	Groundwater flow

✉ Shiliang Liu
shiliangliu@bnu.edu.cn

¹ School of Environment, State Key Laboratory of Water Environment Simulation, Beijing Normal University, Beijing 100875, People's Republic of China

² Safety Evaluation Center, Shenyang Research Institute of Chemical Industry CO., LTD, Shenyang 110021, People's Republic of China

1 Introduction

A variety of factors affect water balance components and hydrological processes, such as landscape composition, soil, topography, climate, and the comprehensive effects of these factors (Li et al. 2016; Tomer and Schilling 2009), in

which recent studies (Kundu et al. 2017; Zhang et al. 2017; Mwangi et al. 2016) have indicated that landscape compositions are one of the most important driving factors in hydrological change. In the process of urban sprawl, artificial landscapes encroach upon large natural landscapes, which results in variations in landscape composition, structure, and pattern (Han et al. 2017). The most obvious characteristic is the increase in impervious surfaces in residential, industrial, and traffic areas (Schütte and Schulze 2017). The occurrence of these large areas alters the runoff coefficient, flow direction, and base flow, and influences hydrological processes further with respect to infiltration, evapotranspiration, and groundwater recharge (Chen et al. 2017; Locatelli et al. 2017). Such changes which are attributable to urbanized landscapes contribute to hydrological disasters, such as floods (Li et al. 2013; Sofia et al. 2017). Further, landscape conversion from forest to artificial surfaces has been shown to change the land–atmosphere energy balance and the water cycle as well (Cuo et al. 2011). Thus, distributions in hydrological processes in rapidly urbanized regions should cause great concern and be considered carefully in urban planning and storm management. Many previous studies have attempted to quantify the effects of landscape change on hydrological processes but the focus however has been primarily on the impacts of landscape types variation on urban rainfall–runoff at finer timesteps. For example, Miller et al. (2014) investigated the changes in storm runoff resulting from the transformation of previously rural landscapes into peri-urban areas and showed an increase in impervious cover accompanied by a reduction of flood duration and increase of peak flood. Yao et al. (2016) explored how imperviousness impacted the urban rainfall–runoff process under various storm cases and implied the increased imperviousness can enhance runoff depth and shorten lag time. Schütte and Schulze (2017) found a strong correlation between different landscape scenarios and hydrological resource flow responses, in that large impervious areas were accompanied by increased stormflows and baseflows. Even within similar landscapes, hydrological components varied remarkably during dry and/or wet years/seasons (Zhang et al. 2015). Andréassian (2004) and Brown et al. (2005) pointed out the increased effects of decreased vegetation cover on annual average discharge. However, few in-depth studies have explored the landscape pattern at spatial–temporal scales and coupled the landscape compositions and landscape pattern indexes with both the hydrological process model and the water balance components at a longer time scale.

In addition, climate change, which can influence the total precipitation volume, frequency of floods, peakflow, and the flow routing time, is another vital driving factor in hydrological processes (Kim et al. 2014; Zhang et al. 2016;

Zhou et al. 2015). It has been reported that more and more frequent extreme weather events have been occurring, together with gradually increasing temperature and precipitation over the past 100 years (NOAA 2016). Global surface temperatures have increased approximately 0.74 °C and have had the direct effects of increasing potential evapotranspiration and decreasing soil moisture (Jeppesen et al. 2016). In urban areas, the “heat island” effect is one of the most obvious climate characteristics and can affect the rainfall mechanism and alter hydrological processes further (Xiao et al. 2005). In addition, precipitation is characterized by unbalanced spatio-temporal distribution, which has resulted in flood and drought risk on regional scales. Many studies have revealed that streamflow and baseflow have an increasing trend under the influences of climate change according to historical records and predictions (Ahiablame et al. 2017; Napoli et al. 2017). Therefore, it is valuable to understand and evaluate the effects of climate change on hydrological processes, particularly the spatio-temporal characteristics of discharge in regional catchments (Zhang et al. 2011).

However, it is difficult to evaluate the individual effect of landscape composition or climate change on hydrological processes because of the complex relationships between human activities and natural meteorological conditions (Mwangi et al. 2016; Nourani and Saeidifarzad 2017). A series of methods, including statistical methods and empirical hydrological models (Li et al. 2009; Putro et al. 2016), have been developed to identify the hydrological response to concurrent nature- and human-induced environmental variations. The statistical method is simple to realize, but lacks a physical mechanism. In contrast, there is a growing interest in various hydrological models that take full account of hydrological factors and spatial parameters to assess the effects of climate change and human activities. For example, Fan and Shibata (2015) found that climate change made a greater contribution to increased surface runoff, lateral flow, and groundwater recharge in the Teshio River watershed using the Conversion of Land Use and its Effects Model (CLUE) and the Soil and Water Assessment Tool (SWAT). Eum et al. (2016) reached similar conclusions using the Cellular Automata model (CA) and Variable Infiltration Capacity model (VIC), and found there was an increasing trend in annual and seasonal flows, which 75% of spring flow was resulted from climate change, while the streamflows in other seasons were affected primarily by land cover changes. In addition, the baseflow from long-term streamflow records (1950–2014) in the Missouri River Basin was assessed by the Web-based Hydrograph Analysis Tool (WHAT), indicating that a 1% increase in precipitation and 1% increase in landscape would lead to an

approximate 1.5% increase and 0.2% decrease in baseflow, respectively (Ahiablame et al. 2017).

Except for the above-mentioned hydrological models, the WetSpa extension, a physically-based and distributed hydrological model, has been adopted to simulate and predict water balance and hydrological processes at the catchment scale (Liu and Smedt 2004). The model aims at not only predicting floods, but also investigating the reasons behind it, especially the spatial distribution of topography, land use, soil type and meteorological conditions (Liu and Smedt 2004). There are several advantages of using the WetSpa extension model. Firstly, the model can be operated at a grid cell scale in variable time-steps (monthly, daily, hourly, and even by minute) and hydrographs can be obtained at different sub-catchment outlets based on long-term water balance. Secondly, it enables simulation of the spatial distribution of hydrological processes, such as runoff, soil moisture, groundwater recharge, etc., and analysis of the land use change and climate change impacts on hydrological processes. Thirdly, the model structure is based on water balance and the parameters are relatively simple. Therefore, the WetSpa extension is suitable for applications at the catchment scale with different sub-catchments. Also, it is suitable for estimating the responses of hydrological processes to climate and landscape heterogeneity.

The relationship between urban landscape pattern and surface water environment are typical for linking studies between pattern and processes. There are close links of material flow and energy flow among different landscape elements in cities, thus significantly affecting urban hydrological characteristics. From the perspective of landscape ecology, based on this relevance, these studies have become a scientific issue with great value. The spatial arrangement of urban landscape patterns and different land use types has proven to be an effective way to improve the regional water environment (Gao et al. 2010). Therefore, the basic principles and methods of landscape ecology were used to explore the hydrological effects, which provides a scientific basis for the recombination of the original landscape pattern or the construction of a new landscape pattern. This landscape approach is the key to realizing the effective control of urban hydrological environments. In China, during urban planning and construction, the design for urban storm water discharge emphasizes the consideration of flood threats, lacking the integration of water environment protection and rainwater resources based on landscape patterns.

The Beiyun River catchment is a major urbanized region and the main water source for residence, agriculture, and industrial development in Beijing (Zhang et al. 2012). In recent decades, the landscape in the region has experienced enormous changes, with rapid urban construction that also

has been accompanied by climate change. As a result, the regional hydrological processes have been altered significantly, especially runoff at the catchment outlet. There are more and more frequent rainstorms in Beijing with the climate change and landscape variation. However, the rain and flood resources can not be effectively used along with shortage of water resources. Previous studies of the Beiyun River have focused primarily on water quality and sources of pollution (Qi et al. 2013; Yang et al. 2012b; Yuan et al. 2014), but few have emphasized the landscape pattern variation and its connection with hydrological processes in Beiyun River. Further, the different sub-catchments have various spatial characteristics related to water balance components. Therefore, it is equally important to explore the features of water quantity and determine the hydrological response to the effects of combined and individual landscape and climate change, which is meaningful for future landscape planning, as well as the development and management of water resources in Beijing.

Therefore, the objectives of our study were to: (1) estimate quantitatively the landscape dynamics of the Beiyun River from 2000 to 2006 and 2006 to 2012 using Sankey diagram method and the landscape index; (2) simulate daily-scale hydrological processes combining landscape pattern and climate, and assess further the spatio-temporal characteristics of discharge based on the WetSpa extension model, and (3) quantify the combined and individual effects of climate and landscape change on surface runoff.

In a theoretical perspective, this study coupled landscape change and the hydrology assessment model, which will be conducive to the regulation of urban landscapes, and will then enrich and develop the relevant theory and technical methods for landscape ecology and urban water environmental protection. In a practical sense, this study will confirm the suitability of the WetSpa hydrological model in Beiyun River, and simulate the hydrological changes over the past 16 years to provide a data basis for future hydrological forecasting. Through the hydrological simulation at sub-basin scale, we can reveal the hydrological processes at different sites, thus providing references for the potential location of sluice gate construction in Beiyun River, which will be helpful for the regulation and control of rainwater flooding, and provide technical support for urban hydrological resource management.

2 Materials and methods

2.1 Study area

The Beiyun River (115°25′–117°30′E, 39°28′–41°05′N) is located between the Chaobai and Yongding Rivers in the

northern area of the North China Plain, and accounts for 26% of the total area of Beijing; it covers 4300 km², has a total length of 120 km, and is a tributary of the Haihe River (Chen et al. 2015). Mountains and hills lie in the northwest and north of this region, with plains in the southern and south eastern areas. The river originates in the Changping and Haidian districts of Beijing city, and flows southwards through Tongzhou district, Xianghe county in Hebei province, and Wuqing county in Tianjin city before joining the mainstream of the Haihe river (Shan et al. 2011). As the most important drainage channel in Beijing, it is responsible for 90% of the discharge of storm-water from the centre of the city and outlying suburbs (Wang et al. 2017). In addition, the Beiyun River connects with many tributaries, including the Shahe, Lingouhe, Qinghe, Bahe, and Tonghui Rivers, the Fenggangjianhe tributaries, and so on, whose floods are collected at different intersections of the mainstream and then flow downstream together (Yang et al. 2012a). Therefore, it presents great challenges for flood control.

The Beiyun river is dominated by a temperate continental monsoon climate, in which rainfall varies continually. Generally, because of the seasonal features of rainfall, approximately 80% of rainstorms occur from June to September, with more than 60% in July and August that are likely associated with the largest flood of the year (Ouyang et al. 2010). With the development of Beijing metropolis, the flow routing conditions in the urbanized river have changed considerably, and to reduce the threat of flooding, many water conservancy measures, such as reservoirs, sluice gates, and rubber dams have been constructed (Ji

et al. 2013; Wang et al. 2017). The study area is shown in Fig. 1.

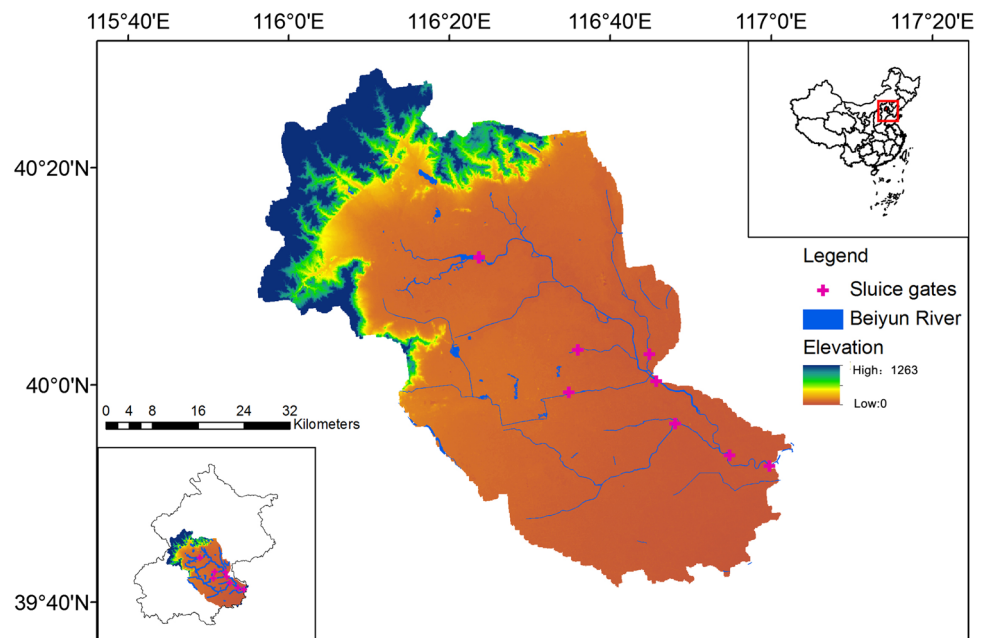
2.2 The study framework

The schematic diagram of the study framework is outlined as below (Fig. 2). Firstly, different data sources were utilized for WetSpa extension model input and landscape characteristics calculation. Secondly, scenarios were setup in the model to discern the effects of landscape change and climate variations in different periods. Finally, the hydrological processes were derived at catchment and sub-catchment scales to reveal the urbanization impact. The details were then described in the following contents.

2.3 Data sources and remote sensing classification

Landscape composition information in the years of 2000, 2006, and 2012 was interpreted using Landsat Thematic Mapper (TM) images (Row 33, Path 123, July–September), with a spatial resolution of 30 m. To meet the model requirements, the landscape types during the three periods were classified into forests (including evergreen needleleaf forest, evergreen broadleaf forest, deciduous broadleaf forest, and mixed forest), shrub, cropland, bare land, grassland, built-up land, and water body. The accuracy of the Kappa statistics for the landscape classifications in 2000, 2006, and 2012 were 0.81, 0.85, and 0.79, respectively. The soil characteristics dataset at a scale of 1:100,000 was obtained from the Environmental and Ecological Science Data Center for West China. The soil

Fig. 1 The study area of Beiyun River



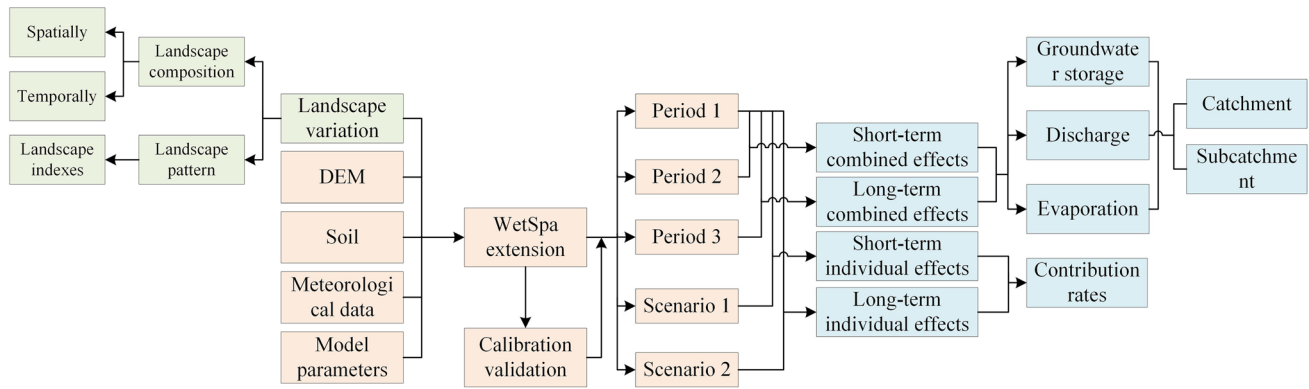


Fig. 2 The framework of our study

classification was then converted into sand, loamy sand, sandy loam, silt loam, loam, and sandy clay loam types. A Digital Elevation Model (DEM) with a resolution of 30 m is available from the Global Land Cover Facility. Time series of precipitation and temperature at six meteorological stations (Beijing, Miyun, Yanqing, Tianjin, Baodi, and Tanggu) around the study region were derived from the Meteorological Data Center of China Meteorological Administration with a 24 h time interval from 2000 to 2016. Discharge series were obtained from a time series of surface water level monitored at 24 h intervals by an automatic data logger at catchment outlet from June to September 2012. Potential evapotranspiration (PET) was calculated by the FAO Penman–Monteith equation as follows (Allen et al. 1998; Allen 2000). Also, these parameters were collected through Meteorological Data Center of China Meteorological Administration.

$$ET_0 = \frac{0.408\Delta(R_n - G) + \gamma \frac{900}{T+273} \mu_2 (e_s - e_a)}{\Delta + \gamma(1 + 0.34\mu_2)} \quad (1)$$

where ET_0 is reference evapotranspiration (mm/day), R_n is net radiation (MJ/m² day), G is soil heat flux density (MJ/m² day), T is air temperature at 2 m height (°C), μ_2 is wind speed at 2 m height (m/s), e_s is saturation vapour pressure (kPa), e_a is actual vapour pressure (kPa), Δ is the slope of the vapour pressure curve (kPa/°C), and γ is the psychrometric constant (kPa/°C). G is presumed to be 0. T_{max} and T_{min} are daily maximum and minimum air temperature.

The data sources of spatial and temporal series were presented in Table 1.

2.4 Measurements of landscape change

To describe the change rate in each landscape composition quantitatively and identify the future change trends, the following landscape dynamic model was introduced to calculate the landscape status with the following equations:

$$V_{in} = \frac{\Delta_{in}}{S_{(i,t1)}} \times \frac{1}{t2 - t1} \times 100\% \quad (2)$$

$$V_{out} = \frac{\Delta_{out}}{S_{(i,t1)}} \times \frac{1}{t2 - t1} \times 100\% \quad (3)$$

$$D_i = \frac{V_{out} + V_{in}}{V_{out} - V_{in}} \quad (-1 \leq D \leq 1) \quad (4)$$

where Δ_{in} is the area of newly-formed landscape i converted from other landscape types; Δ_{out} is the area of landscape i converted into other landscape types; $S_{(i,t1)}$ is the area of landscape i in year $t1$; V_{in} and V_{out} are the rates of increase and decrease from $t1$ to $t2$; D_i is the status index of landscape i , in which $-1 \leq D \leq 0$ indicates that the landscape i has a trend of expansion, and the higher the D_i , the greater the likelihood of expansion. In contrast, the area of landscape i may reduce constantly with $0 \leq D \leq 1$ (Xian et al. 2005).

In addition, increasing numbers of researchers are adopting landscape indices to elaborate the ecological processes associated with the development of urban expansion (Li et al. 2015a; Su et al. 2012; Xiao et al. 2013). Through analysis of these indices, complex and unclear spatial landscape characteristics can be quantified so that they may be identified effectively. In general, the choice of landscape indices needs to meet the following criteria: (1) feasible to reflect the landscape pattern characteristics of the study area; (2) able to be ecologically significant; (3) comparable to previous landscape ecological studies, and (4) less redundancy among different landscape indices (Su et al. 2012, 2014). Based on these criteria, we selected a set of indices calculated by the moving window method with a window size of 500 m using Fragstats 4.2, which indicates landscape diversity, heterogeneity, fragmentation level, and shape information for the Beiyun River basin. The computational formulas and ecological meanings of selected landscape indexes are shown in Table 2. Patch Density (PD) and the Largest Patch Index (LPI) were used

Table 1 Summary of data in the study

Data	Period	Source
Geo_spatial data		
Landscape	2000, 2006, 2012	Landsat Thematic Mapper (TM) images (Row 33, Path 123) http://glcfapp.glcf.umd.edu:8080/esdi/index.jsp
Soil	2000	Environmental and Ecological Science Data Center for West China http://www.soil.csdb.cn/
DEM	2000	Global Land Cover Facility http://gdem.ersdac.jspacesystems.or.jp/
Temporal data		
Precipitation	2000–2016	Meteorological Data Center of China Meteorological Administration http://data.cma.cn/data/cdcindex/cid/6d1b5efbdcfb9a58.html
Temperature	2000–2016	
PET parameters	2000–2016	
Discharge	2012.06-09	Surface water level monitor

Table 2 Selected landscape indices and their ecological meanings

Landscape indices	Abbreviations	Calculation formula	Ecological meanings
Patch density	PD	$PD = N/A$	The larger the PD value, the more severe the degree of fragmentation
Largest Patch Index	LPI	$LPI = \left[\frac{\max(a_{ij})}{A} \right]$	The LPT describes the dominant types of landscape
Aggregation Index	AI	$AI = \left[\sum_{i=1}^m \left(\frac{g_{ii}}{\max - g_{ii}} \right) P_i \right]$	AI increases with the more concentrated patch types
Splitting Index	SPLIT	$SPLIT = \frac{\sum_{i=1}^m A_i^2}{\sum_{i=1}^m \sum_{j=1}^m a_{ij}^2}$	The SPLIT value reflects the subdivision degree of a landscape
Area Weighted Shape Index	SHAPE-AM	–	The larger the SHAPE-AM, the more complex the shape of patch
Edge density	ED	$ED = \frac{1}{A} \sum_i e_{ik} \times 10000$	The higher the ED, the longer the edge between different patches
Patch Cohesion Index	COHESION	$COHESION = \left[1 - \frac{\sum_{i=1}^m p_{ij}}{\sum_{j=1}^m p_{ij} \sqrt{a_{ij}}} \right]$	The different landscape types have better connectedness with larger COHESION
Shannon’s Diversity Index	SHDI	$SHDI = - \sum_{i=1}^n p_i \times \ln p_i$	SHDI implies the abundance and distribution of different landscape types

N = total number of patches in the landscape; A = total landscape area; a_{ij} = area of patch ij ; m = number of patch types (classes) in the landscape; P_i = proportion of the landscape occupied by patch type (class) i ; g_{ii} = number of like adjacencies (joins) between pixels of patch type (class) i ; e_{ik} = the edge length between patch i and k ; p_{ij} = the perimeter of patch ij

to demonstrate information about landscape fragmentation. Aggregation Index (AI) and Splitting Index (SPLIT) were used to quantify the adjacencies among different patches. Area Weighted Shape Index (SHAPE-AM) and Edge Density (ED) were used to measure shape and size information, and Patch Cohesion Index (COHESION) was employed to display physical connectedness. Shannon’s Diversity Index (SHDI) reflects the patch abundance and heterogeneity in the landscape (Liu et al. 2017; McGarigal et al. 2002; Zhao et al. 2012).

2.5 WetSpa extension model for hydrological simulation

The WetSpa extension, developed by Wang et al. (1996), is a physically-distributed hydrological model designed to predict the water and energy transfer between soil, plants, and atmosphere at catchment scale which was improved subsequently by Liu and Smedt (2004). In order to deal with the heterogeneity, the model was executed at a grid scale and each grid was further divided into vegetation cover and bare soil. For each grid, the simulated hydrological system covers four parts: plant canopy, soil surface,

root zone in soil and groundwater. The structure of WetSpa extension at a grid level is shown in Fig. 3. It takes into account the processes of precipitation, interception, surface runoff, depression, infiltration, interflow and recharge. Firstly, rainfall is intercepted by canopy before reaching the ground surface. Next, the remaining water fills the depression storage, runs off, or infiltrates into soil depending on the intensity of precipitation, landscape types, elevation, and soil texture. The infiltrated portion is able to fill the soil moisture in the root zone, flow as interflow, or percolate into the groundwater storage lengthwise. The total runoff at a grid scale consists of the surface runoff, the interflow and the groundwater flow. The water balance for the groundwater storage includes groundwater recharge, deep evapotranspiration, and lateral groundwater flow. Evapotranspiration takes place in each section of the plant, the intercepted and depressed water, and soil surface (Liu and Smedt 2004).

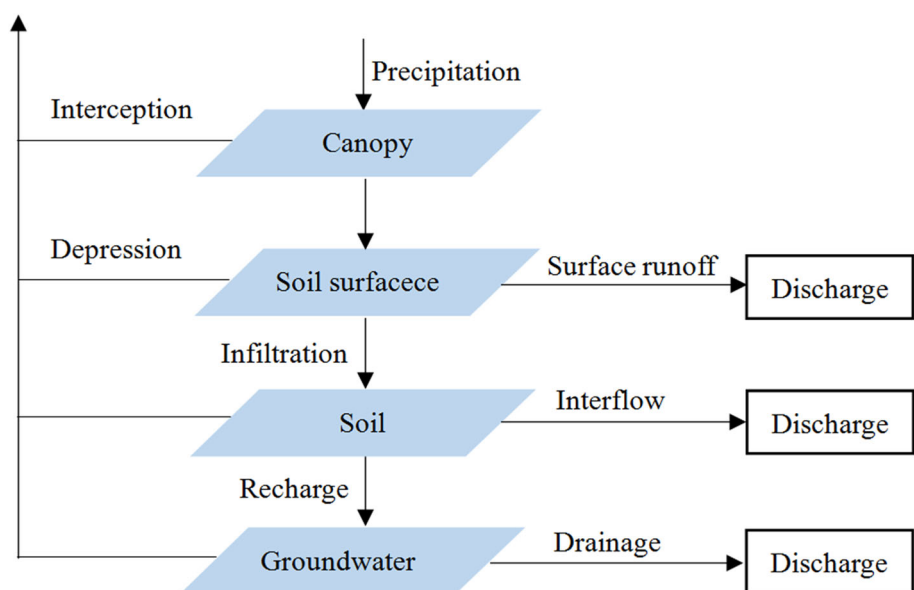
Running the WetSpa extension at catchment scale requires the preparation of a spatial database for deriving model parameters. Landscape types, soil texture, and elevation are three basic types. In addition, other digital data, such as shape file of gauging station locations, stream network, major traffic lines boundary and sewer systems, are optional depending on the data available and the purpose and accuracy requirement of the project. These data are useful to delineate path network for watershed drainage, estimate spatial rainfall distribution, and determine the model routing parameters. Also, the hydro-meteorological data, mainly including precipitation, potential evapotranspiration and discharge at a certain time-step, are basic inputs for WetSpa extension. Temperature data are

required when snowmelt occurred in the study area and periods.

In the model, there are some default parameters for landscape types, soil texture, potential runoff coefficient and depression storage capacity. In addition, 12 global parameters, including the interflow scaling factor (K_i), rainfall degree-day coefficient (K_{rain}), groundwater recession coefficient (K_g), initial groundwater storage (G_0), the correction factor of PET (K_{ep}), temperature degree-day coefficient (K_{snow}), initial soil moisture (K_{ss}), base temperature for snowmelt (T_0), the rainfall intensity (P_{max}), and surface runoff exponent (K_{run}), are employed in WetSpa extension to simplify the process of parameter calibration and simulate the hydrological processes realistically (Liu et al. 2003). It is preferable to calibrate 12 global parameters against observed runoff data rather than adjust the spatial parameters.

To assess how well the model simulates the hydrological processes, model bias (CR1), model confidence (CR2) and Nash–Sutcliffe efficiency (E_{ns}) between simulated and observed surface runoff were adopted (Nash and Sutcliffe 1970; Verbeiren et al. 2013). The model bias shows the gap between model expectation and real value, which can reflect the systematic accuracy and the ability of reproducing water balance. Model confidence represents the proportion of the variance in the observed discharges that are explained by the simulated discharges. Nash–Sutcliffe efficiency is used for evaluating how well the hydrological processes are simulated by the model and describes the ability of reproducing the time evolution of discharge. The calculation formulas are as follows:

Fig. 3 Structure of WetSpa extension



$$CR1 = \frac{\sum_{i=1}^n (Q_s - Q_o)}{\sum_{i=1}^n Q_o} \quad (5)$$

where CR1 is the model bias, Q_s and Q_o are the simulated and observed discharge at the same time (m^3/s). The CR1 is lower, the fit is better. CR1, which is zero, shows the perfect simulation.

$$CR2 = \frac{\sum_{i=1}^n (Q_s - Q_{o_ave})^2}{\sum_{i=1}^n (Q_o - Q_{o_avg})^2} \quad (6)$$

where CR2 is the model determination coefficient with range from 0 to 1. When CR2 is close to 1, it indicates a high level of model confidence. Q_{o_ave} is the mean observed discharge in the study period.

$$E_{ns} = 1 - \frac{\sum_{i=1}^n (Q_o - Q_s)^2}{\sum_{i=1}^n (Q_o - Q_{avg})^2} \quad (7)$$

where E_{ns} is the Nash–Sutcliffe efficiency and less than 1. When the value is close to 1, it indicates a better fit between the simulated and observed discharge.

In general, a model that meets the requirement of $CR1 < 20\%$, $CR2 > 0.6$ and $E_{ns} > 0.5$ can be used for prediction.

After calibration, the model was validated with correlation coefficient (R^2) between simulated and observed discharge at the same time. The operation processes can be seen in Fig. 4.

2.6 Scenario analysis

For WetSpa extension, it is able to simulate the spatio-temporal hydrological processes of precipitation, evapotranspiration, runoff, groundwater, interception, infiltration, interflow, percolation, and depression, among others, on a monthly, daily, or hourly scale based on the water balance of each grid cell. Further, it can analyze the effects of landscape variation and climate change on hydrological processes, especially the discharge of the entire catchment and sub-catchment outlets (Liu and Smedt 2004)). Considering the heterogeneity in the study area, the WetSpa extension runs at grid cell scale with a size of $100\text{ m} \times 100\text{ m}$ in the Beiyun River basin.

Among all of the water balance components (interception, infiltration, evapotranspiration, percolation, runoff, and groundwater storage), the runoff varied significantly based on the combined influences of rainfall and landscape compositions in the process of urban expansion. Therefore, runoff was used to quantify the response to climate change and landscape composition variation. As landscape change experiences a greater temporal scale than the climate variation interval, we divided the study period into three phases, 2000–2005 (period 1), 2006–2011 (period 2), and

2012–2016 (period 3). To discern the effects of landscape and climate changes on runoff, two other scenarios were set for comparison, in which the landscape in 2000 was kept constant as the base period accompanied by climate data from 2006–2011 and 2012–2016, respectively. Comparing period 2 and 3 with period 1, we can understand the way in which the runoff was influenced by the combined climate and landscape composition changes during the two phases. Further, the contribution rates of individual climate change to runoff can be identified by comparing scenarios 1 and 2 with period 1 (Table 3).

3 Results

3.1 The landscape dynamics in Beiyun River basin

3.1.1 The landscape spatial–temporal compositions of Beiyun River basin in different periods

The spatial characteristics of landscape information in 2000, 2006 and 2012 were presented in Fig. 5. It is clear that the landscape types in the Beiyun River varied greatly during the 13 years. The built-up land was gradually expanding into upstream and downstream in Beiyun River basin. In order to explore the landscape dynamics of each landscape type in three periods, a Sankey diagram was drawn to show the transformations of the different landscape types from 2000 to 2006 and from 2006 to 2012 (Fig. 6). With a cover of 42.5%, cropland was the largest landscape type in 2000. However, it experienced a significant loss from 2000 to 2006, in which 260 km^2 , 202 km^2 , and 60 km^2 of croplands were converted into built-up land, forest, and grassland, respectively. As a result, the total cropland area decreased to 32.1% in 2006, and then subsequently to 26.4% in 2012. Built-up land demonstrated the opposite trend and became the dominant type in 2012 as the result of urban encroachment on cropland, which increased 6.2% from 2000 to 2006, and 4.4% from 2006 to 2012. With respect to forests, a small percentage was converted into built-up land and cropland, while more significant changes took place in which cropland was converted to artificial forests from 2000 to 2006. Finally, forest cover reached 21.6% of the total area of the Beiyun River basin in 2012. Shrub land maintained a steady state, with an average cover of 6.4% during the three periods. Although grassland had the minimum proportion of 1% in 2000, it also changed significantly, and increased more than three times during the 13 years.

To quantify the changes in different landscape compositions further, we adopted the status index (D_i) based on the transfer rate of each landscape type to analyze their

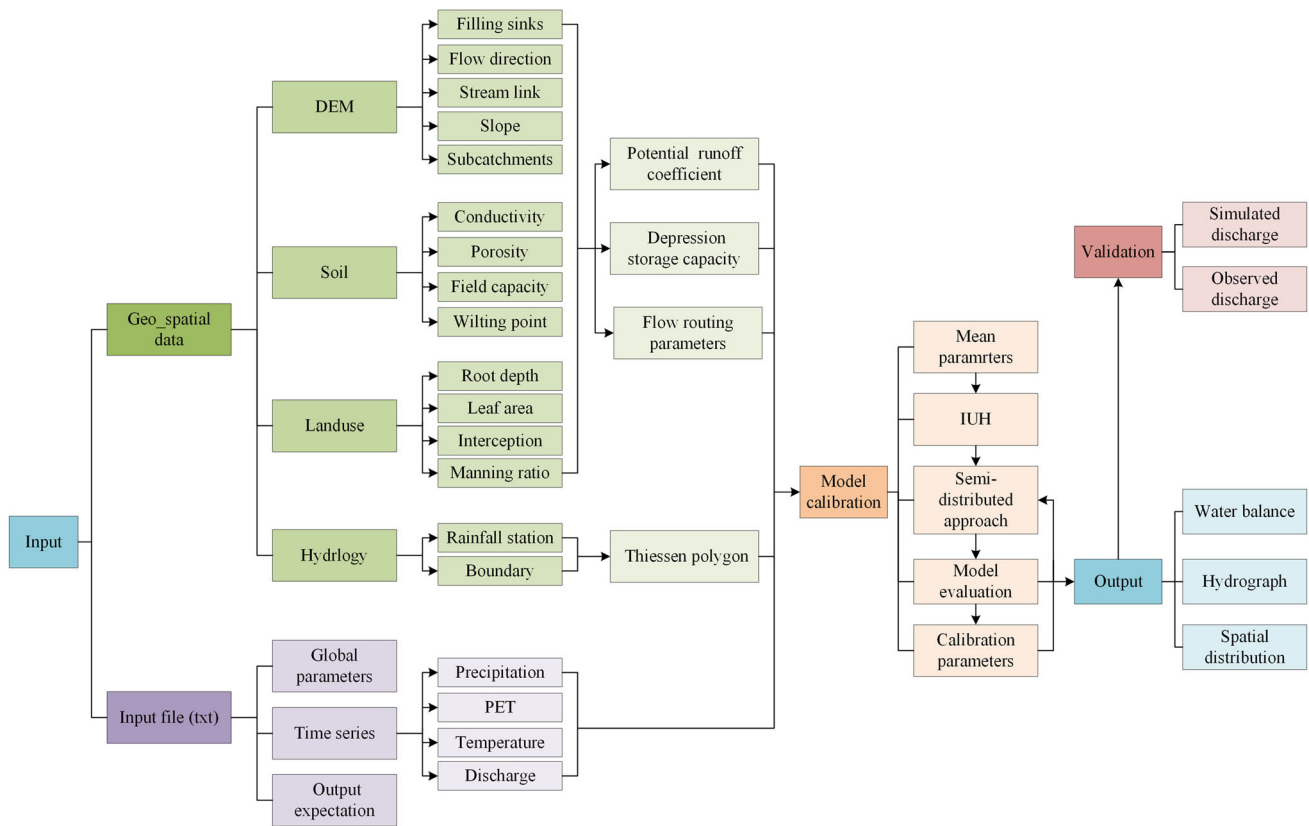


Fig. 4 The special operation processes for WetSpa extension

Table 3 Different scenarios for modeling analysis

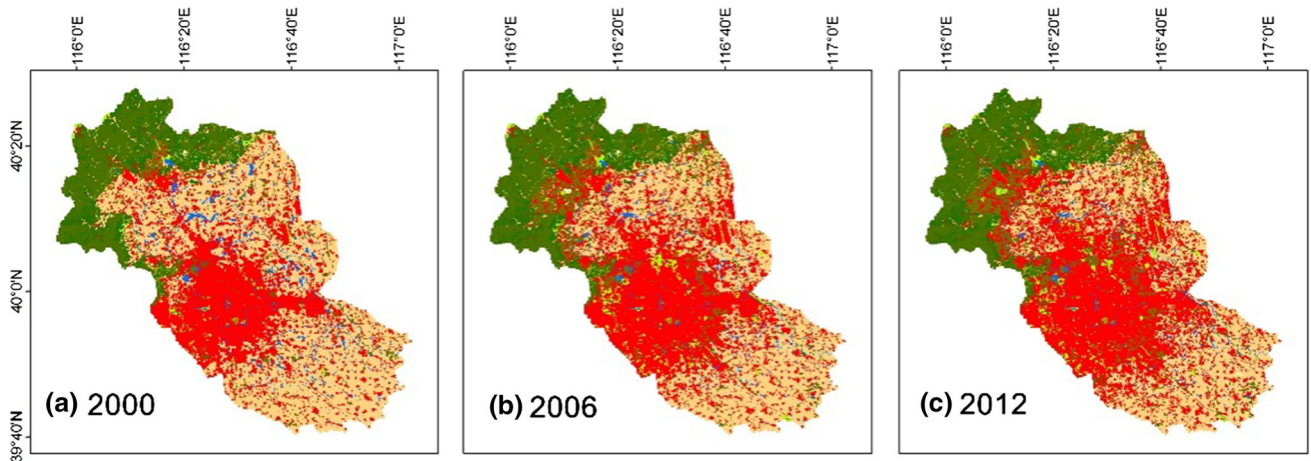
Number	Comparison	Base landscape status	Meteorological data
1	Period 1	2000	2000–2005
2	Period 2	2006	2006–2011
3	Period 3	2012	2012–2016
4	Scenario 1	2000	2006–2011
5	Scenario 2	2000	2012–2016

future change trends. The results in Table 4 showed that the D_i of cropland and water body was -0.82 and -0.67 , indicating that those landscape types most likely will continue to decline. D_i of other types, such as evergreen broadleaf forest, mixed forest, grassland, and built-up land, were all greater than 0.60 , indicating an increasing trend in the future, in which grassland had the largest transfer rate.

3.1.2 Landscape pattern variations in two periods

Further results of landscape patterns characterized by the selected indices are shown in Table 5. LPI changed from 80.31 to 79.03 from 2000 to 2006, and to 77.75 in 2012, indicating that the percentage of total area of largest patch

declined and some large patches became fragmented. Correspondingly, the lengths of all edge segments reflected by ED in the Beiyun River catchment increased in 2006 and 2012. The shape characteristics also increased constantly, with SHAPE-AM changing from 1.12 to 1.14 and 1.15 , suggesting that the shape of different landscape types in the catchment became more unstable and irregular when urban landscapes gradually expanded. In addition, the most obvious change was accompanied by landscape fragmentation, with an increase in PD from 9.05 to 9.39 and 9.76 . The increase in SPLIT and decrease in AI also demonstrated the fragmentation level in the Beiyun River catchment, signifying that the landscape in the urbanized region tends to be more isolated and less aggregated. Accompanied by the landscape fragmentation in the process of urban development, landscape diversity also made some responses to the change, in which single and natural landscape patterns have been replaced by mixed and artificial landscape patterns. As a result, SHDI increased from 0.41 to 0.46 in the 13 years, indicating that the richness and evenness of the landscape increased. Meanwhile, COHESION decreased slightly by 1.09 with decreased landscape connectivity.



Legend

- Evergreen Needleleaf Forest
- Deciduous Broadleaf Forest
- Shrub
- Cropland
- Bare land
- Evergreen Broadleaf Forest
- Mixed Forest
- Grassland
- Built-up land
- Water Body

Fig. 5 The landscape types of Beiyun River in 2000, 2006, and 2012

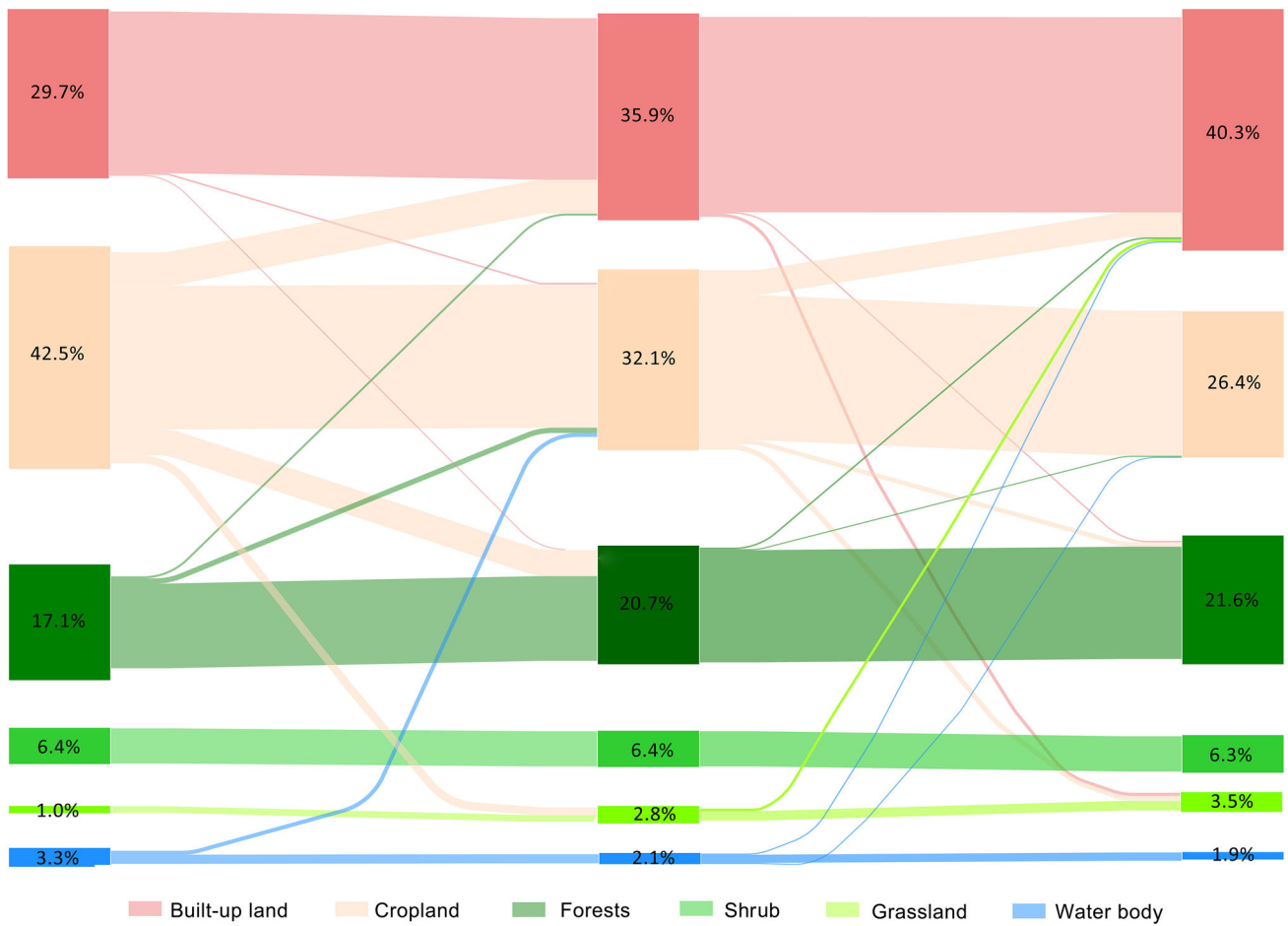


Fig. 6 The dynamics of different landscape types in the Beiyun River from 2000 to 2006, and 2006 to 2012

Table 4 The status index of different landscape compositions

Landscape composition	2000 (km ²)	2012 (km ²)	V_{in}	V_{out}	D_i
Evergreen needleleaf forest	32.61	33.34	1.33	0.63	0.35
Evergreen broadleaf forest	134.60	316.29	232.18	51.21	0.64
Deciduous broadleaf forest	562.39	568.98	36.71	30.00	0.10
Mixed forest	4.21	7.19	3.24	0.36	0.80
Shrub	276.62	271.62	4.72	9.59	− 0.34
Grassland	38.07	144.51	111.20	8.82	0.85
Cropland	1826.27	1133.38	75.77	774.03	− 0.82
Built-up land	1278.21	1733.32	509.96	47.60	0.83
Bare land	3.07	10.36	8.21	1.04	0.78
Water body	143.39	80.45	15.05	75.09	− 0.67

Table 5 The change in landscape indices during the three periods

Landscape indices	2000	2006	2012
LPI	80.31	79.03	77.75
ED	23.82	25.66	27.51
SHAPE-AM	1.12	1.14	1.15
PD	9.05	9.39	9.76
SPLIT	1.57	1.61	1.66
COHESION	91.58	91.05	90.49
AI	91.73	90.82	89.99
SHDI	0.41	0.43	0.46

In conclusion, the landscapes in this region are prone to be disaggregated, fragmented, and complicated because of urbanization.

3.2 The effects of climate change and landscape variation on hydrological processes based on the WetSpa extension

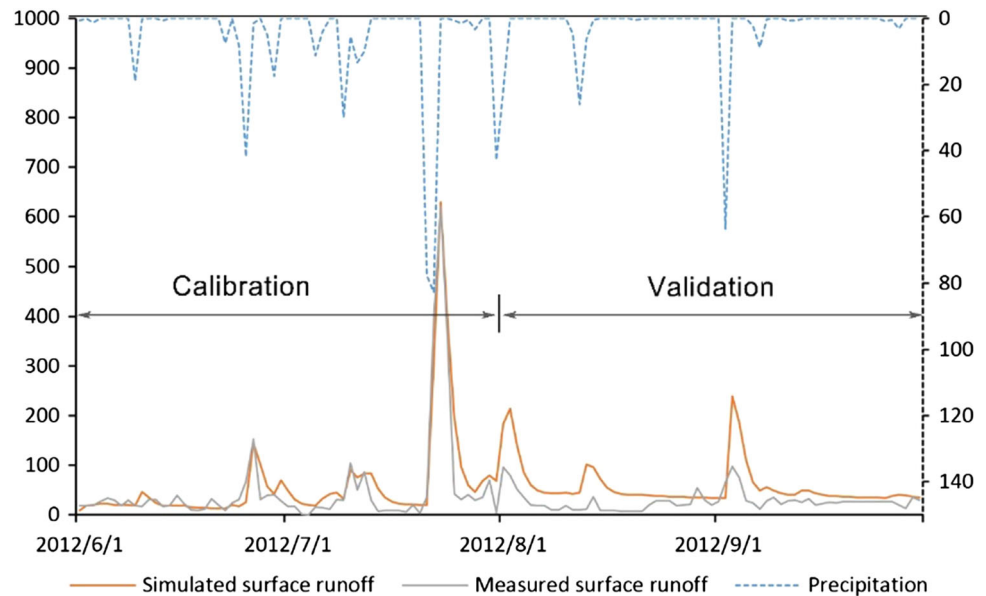
3.2.1 Calibration and validation of the WetSpa extension

Calibration and validation of the WetSpa extension are vital steps in obtaining optimal results in the evaluation of hydrological processes. The periods from June 1, 2012 to July 31, 2012 were used for model calibration for this region, while model validation was performed for the period from August 1, 2012 to September 30, 2012. Through a combination of manual and auto-calibration, the global parameters were finally determined as follows: interflow scaling factor (K_i) = 1.2; groundwater flow recession coefficient (K_g) = 0.01 m²/s; soil moisture ratio (K_{ss}) = 0.8977; correction factor for PET (K_{ep}) = 1.0022; initial groundwater storage in depth (G_0) = 45 mm; base temperature (T_0) = 0.55 °C; temperature degree-day coefficient for calculating snowmelt (K_{snow}) = 1.43 (mm/°C/day); rainfall degree-day

coefficient (K_{rain}) = 0.002 (mm/mm/°C/day); exponent reflecting the effect of rainfall intensity on the actual surface runoff coefficient (K_{run}) = 1.98, and threshold of rainfall intensity in mm/day (P_{max}) = 500 mm. Based on current global parameters and spatial data, model evaluation indicated Nash–Sutcliffe efficiency reached 0.71, implying the simulation results from the model coincided generally with the actual discharge in this region. Model determination coefficient was 0.84, indicating a high level of model confidence. However, the relative error between simulated and observed runoff volume reached 18%, and as a whole, the simulated values were higher than those observed. The reality is that there are several sluice gates in the Beiyun River that could intercept discharge and the WetSpa extension is not able to evaluate the effects of sluice gates on the runoff column. In general, the results of WetSpa extension calibration can meet the requirement for hydrological simulation and scenario analysis in Beiyun River.

The model validation is used to verify the calibrated model parameters through comparing the simulated and observed discharge in the period from August 1, 2012 to September 30, 2012. The hydrographs of simulated and observed runoff volumes and precipitation of the Beiyun River on daily scale for model validation are shown in Fig. 7. Both of the two runoffs demonstrated similar changing trends and also made hysteresis responses to the rainfall. Although the observed runoff volumes are not available for every peak flow of the simulated values, there was still good agreement between the two hydrographs. Five heavy storms occurred on June 26, July 10 and 23, August 1, and September 3, with observed discharges of 153, 104, 620, 96, and 98 m³/s, respectively. Correspondingly, the simulated flood peaks were 144, 91, 629, 183, and 189 m³/s. In addition, we adopted correlation coefficient (R) to verify the capabilities of the WetSpa extension. The correlation coefficient between simulated and observed values was greater than 0.80, reflecting small differences generated by the hydrological model and the

Fig. 7 Calibration and validation of the WetSpa extension



calibrated model parameters were applicable to Beiyun River.

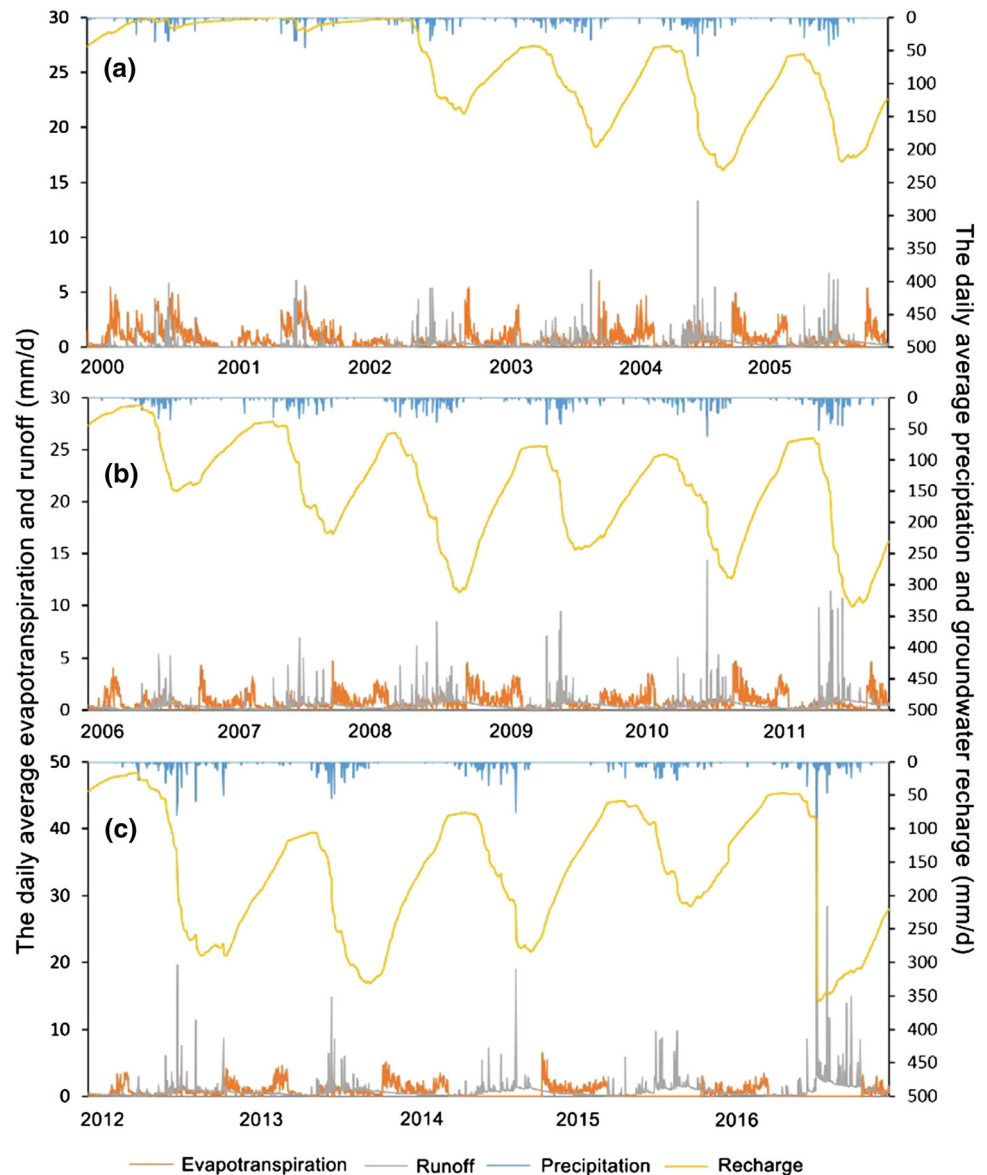
3.2.2 Hydrological processes of water balance components

The WetSpa extension model considers the comprehensive effects of landscape composition, precipitation, soil texture, and elevation on hydrological processes. In the short term, soil texture and elevation are stable. Therefore, we explored primarily the way in which the water balance components (interception, infiltration, evapotranspiration, percolation, runoff, and daily active groundwater storage) changed due to the combined influences of variations in precipitation and landscape composition. Combining landscape types in 2000, 2006, and 2012 with continuous daily average meteorological data from 2000 to 2005, 2006 to 2011, and 2012 to 2016, respectively, we constructed three hydrographs of precipitation and water balance components (Fig. 8). Overall, precipitation from period 1 to 3 showed an increasing trend accompanied by increasing runoff and groundwater storage, while they had different “high-low” orders during the same period. The annual average runoff values were 46.3 mm, 62.8 mm and 123.8 mm when the daily average groundwater storages were 73.2 mm, 144.8 mm and 192.1 mm in three periods, respectively. During period 1, the annual average rainfall was 395 mm in 2000, and the simulated average interception (I), infiltration (F), actual evapotranspiration (Et), percolation out of root zone (Perc), and total runoff (R) losses were 15 mm, 348 mm, 434 mm, 29 mm, and 66 mm, respectively. At the same time, the average daily active groundwater storage at this time-step was 13 mm. However, beginning from 2002, the average annual rainfall

demonstrated an increasing trend, with a maximum of 503 mm in 2004. Correspondingly, it maximized the total runoff and daily active groundwater storage of 189 mm and 128 mm, respectively.

Similarly, the water balance conditions for the entire catchment from 2006 to 2011 during period 2 (Fig. 8b) and from 2012 to 2016 in period 3 (Fig. 8c) were derived. Comparing Fig. 8a, b, it is evident that the differences in hydrological processes were caused primarily by changes in landscape composition and rainfall. The quantitative analysis of landscape compositions from 2000 to 2006 is elaborated in Fig. 6 and Table 4. During period 2, the average annual precipitation from 2006 to 2011 was 364 mm, 472 mm, 601 mm, 451 mm, 532 mm, and 604 mm, respectively. Heavy rains occurred more frequently in 2008 and 2011. As a result, most of the water balance components were higher during period 2 than those during period 1. Particularly in 2011, the average interception (I), infiltration (F), actual evapotranspiration (Et), percolation out of root zone (Perc), and the total runoff (R) losses reached 7 mm, 497 mm, 291 mm, 354 mm, and 249 mm, respectively. With respect to period 3, the cumulative rainfall over the years continued to increase. All average annual rainfalls from 2012 to 2016 were greater than 500 mm, except that in 2015, with a minimum value of 438 mm. In 2016, the total runoff and average active groundwater storage reached new peaks of 541 mm and 349 mm, respectively. Although, the annual average rainfalls of 503 mm in 2004 and 504 mm in 2015 were almost equal, the differences in water balance components remained great because of the effect of landscape composition. In particular, the total runoff column of the Beiyun River in 2015 was almost twice that in 2004.

Fig. 8 The hydrological processes during different time periods based on the WetSpa extension (**a** period 1; **b** period 2; **c** period 3)



3.2.3 Discharge at the entire catchment and different subcatchment outlets

The total discharge at the entire catchment outlet consists of surface runoff (Q_s), interflow (Q_i), and groundwater flow (Q_g). Their distribution characteristics from 2000 to 2016 for time periods 1–3 are shown in Fig. 9. At the same time-step (24 h), surface runoff and groundwater flow accounted for a large proportion, while interflow was relatively small. The total runoff exhibited an increasing trend from 2000 to 2005, with the lowest level of 12.8 mm/day in 2001, and the highest level of 75 mm/day in 2004. Further, surface runoff and groundwater runoff exhibited similar trends. From 2006 to 2011, the average daily discharge fluctuated slightly at approximately 35 mm, with a surface runoff of 20 mm and groundwater runoff of

approximately 15 mm. However, the average daily total discharges from 2012 to 2016 reached a higher level than those during periods 1 and 2, and increased over years. The minimum value was higher than 50 mm/day, while the maximum, 98.7 mm/day, occurred in 2016, with surface runoff of 64.7 mm/day and groundwater runoff of 31.8 mm/day attributable to a rainstorm event throughout the entire catchment.

At the subcatchment scale, the discharges possessed obvious characteristics of spatial distribution with different landscape compositions, precipitations, elevations, and soil textures in the three time series shown in Fig. 10. Generally, the runoffs within the eight sub-catchments exhibited similar change trends from 2000 to 2016. In upstream sub-catchments, the annual average discharges for Shahe and Lingouhe were $0.43 \text{ m}^3/\text{s}$ and $0.16 \text{ m}^3/\text{s}$ in 2000,

Fig. 9 Discharges at the catchment outlet during different time periods under different landscape composition and climate conditions (**a** period 1; **b** period 2; **c** period 3)

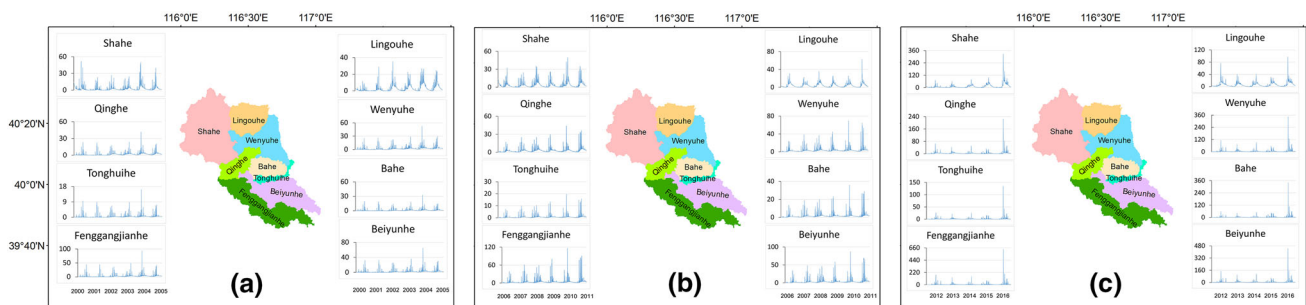
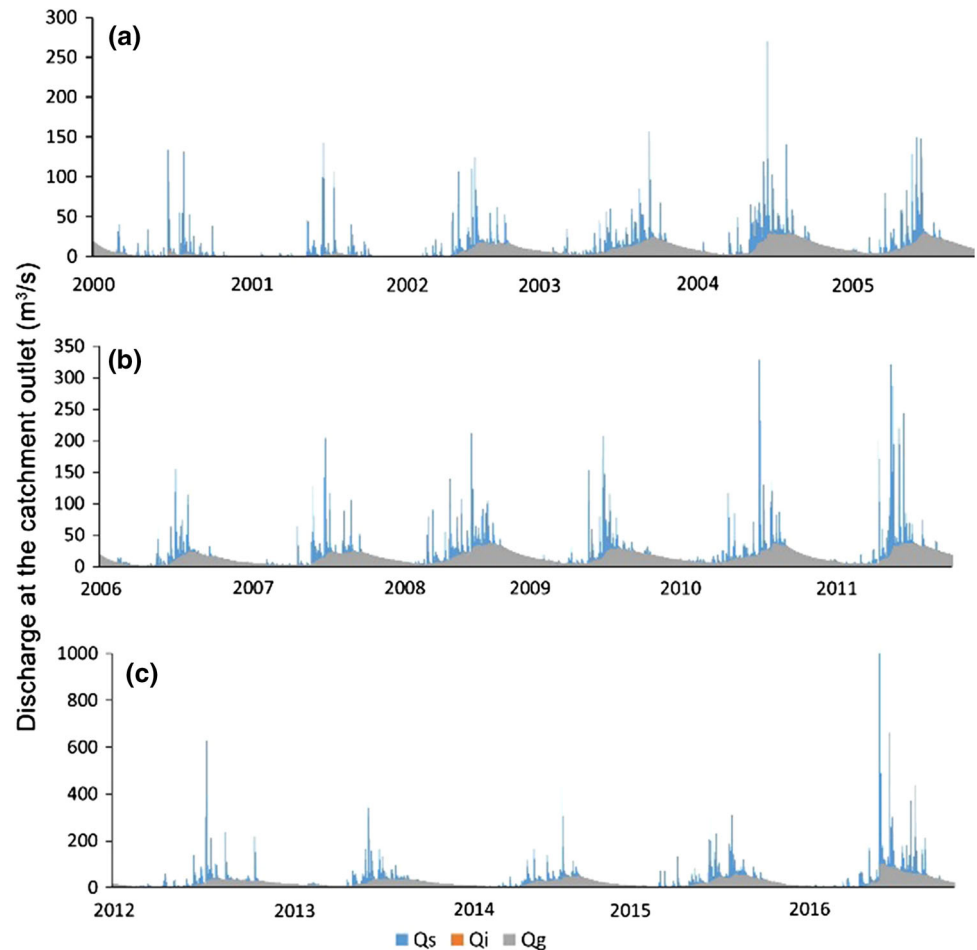


Fig. 10 Discharge at different subcatchment outlets during different time periods (**a** period 1; **b** period 2; **c** period 3)

respectively. In mid-stream sub-catchments, the discharges for Qinghe, Wenyuhe, Bahe, and Tonghuihe increased to approximately $2.5 \text{ m}^3/\text{s}$. However, where the river flows downstream of Beiyunhe and Fenggangjianhe, the average discharges dropped considerably to approximately $0.8 \text{ m}^3/\text{s}$. From 2000 to 2005, all sub-catchments had the maximum runoff in 2004. In the second time series, the discharges in all sub-catchments were higher from 2006 to 2011, ordered mid-stream > downstream > upstream. The maximum average discharges in different sub-catchments occurred in Lingouhe in 2008, with $4.8 \text{ m}^3/\text{s}$, Qinghe with

$3.8 \text{ m}^3/\text{s}$, and Fenggangjianhe with $4.5 \text{ m}^3/\text{s}$, respectively. In the third time series, the discharges in different sub-catchments increased clearly over years. In detail, runoffs in Shahe, Lingouhe, Wenyuhe, Qinghe, Bahe, Tonghuihe, Beiyunhe, and Fenggangjianhe from 2012 to 2016 ranged from $5.6\text{--}21.9 \text{ m}^3/\text{s}$, $4.9\text{--}7.4 \text{ m}^3/\text{s}$, $3.8\text{--}7.3 \text{ m}^3/\text{s}$, $2.7\text{--}5.5 \text{ m}^3/\text{s}$, $1.6\text{--}4.3 \text{ m}^3/\text{s}$, $0.6\text{--}1.5 \text{ m}^3/\text{s}$, $3.5\text{--}7.9 \text{ m}^3/\text{s}$, to $4.0\text{--}8.8 \text{ m}^3/\text{s}$, respectively. In summary, the hydrographs for the sub-catchments not only illustrate the runoff processes in different periods, but also explore the spatio-

temporal distribution of high runoff production in the Beiyun River.

3.3 The contribution rates of climate change and landscape variation to surface runoff

According to the comparison, the responses of surface runoff to climate change and landscape variation in different time periods were derived quantitatively. Period 1 was considered as the base period. Scenarios 1 and 2 eliminated the effects of landscape change on runoff during the period from 2006 to 2011 and from 2012 to 2016, respectively. The results indicated that the annual average precipitation during periods 1, 2, and 3 were 418.5 mm, 504 mm, and 570.4 mm, when yearly average surface runoffs reached 46.3 mm, 62.8 mm, and 123.8 mm, respectively (Table 6). From period 1 to period 2, the total surface runoff due to combined influence of landscape composition variation and climate change increased 16.5 mm. It is worth noting that the individual climate change had a positive effect and resulted in an increase of runoff with 19.9 mm while the individual landscape variation had a negative effect and resulted in a decrease of runoff with 3.4 mm at the same time period. Therefore, the contribution rates of climate and landscape changes to surface runoff were + 120.6% and – 20.6%, respectively. At longer time scale, the total surface runoff due to combined influence of landscape composition variation and climate change increased 77.5 mm from period 1 to period 3. Differently, the individual climate change and landscape variation both had positive effects to increased runoff. Specifically, the runoff increased 72.6 mm and 4.9 mm due to the individual effect of climate change and landscape variation, respectively.

Correspondingly, the contribution rate of climate change to surface runoff dropped to 93.6%, while it rose to 6.4% because of the effects of variations in landscape composition. The results above indicated that landscape composition variation during 2006–2011 decreased runoff, while it

increased runoff during 2012–2016. In contrast, climate change was always the dominant factor and increased runoff during both periods.

4 Discussion

4.1 The effects of human-induced variation in landscape composition on hydrological processes

In our study, the changing trends in groundwater storage and runoff can be attributed to the interference of human activities on the landscape, particularly the conversion of cropland to built-up land.

During the period from 2006 to 2011, the individual landscape variation decreased runoff compared to the period from 2000 to 2005. In this period, water intake with the development of agriculture and industry in the Beiyun River catchment resulted in a significant reduction of fluvial streamflow. Further, afforestation and returning cropland to forests enhanced water and soil conservation. As a result, human-induced landscape variation decreased annual average streamflow. However, with the increase of human activities, the area of built-up land exceeded those of cropland and forests, and led to lower runoff coefficients in 2012. Overall, the individual landscape change during the 13 years accounted for a 6.4% increase in runoff.

In addition, some current studies have noted that different spatial patterns of landscape composition alter water distribution. Liu and Shi (2017) found a significant correlation between streamflow and the proportion of residential land. Greater population density and building areas increase the vulnerability to floods and produced further flood hazards. Moreover, Napoli et al. (2017) suggested that artificial surfaces and agriculture have played vital roles in the increase in peak flow and total runoff. In contrast, Zhou et al. (2013) reported that the land use change attributable to urbanization caused the base flow to

Table 6 The quantitative effects of precipitation and landscape variation in 2006–2011 and 2012–2016 based on the reference period of 2000–2005

Comparison	Average precipitation (mm)	Average runoff (mm)	Total variation for runoff (mm)	Runoff variation caused by rainfall (mm)	Contribution of rainfall (%)	Run variation caused by landscape (mm)	Contribution of landscape (%)
Period 1	418.5	46.3	–	–	–	–	–
Period 2	504.0	62.8	16.5	–	–	–	–
Period 3	570.4	123.8	77.5	–	–	–	–
Scenario 1	418.5	66.2	–	19.9	120.6	– 3.4	– 20.6
Scenario 2	418.5	118.9	–	72.6	93.6	4.9	6.4

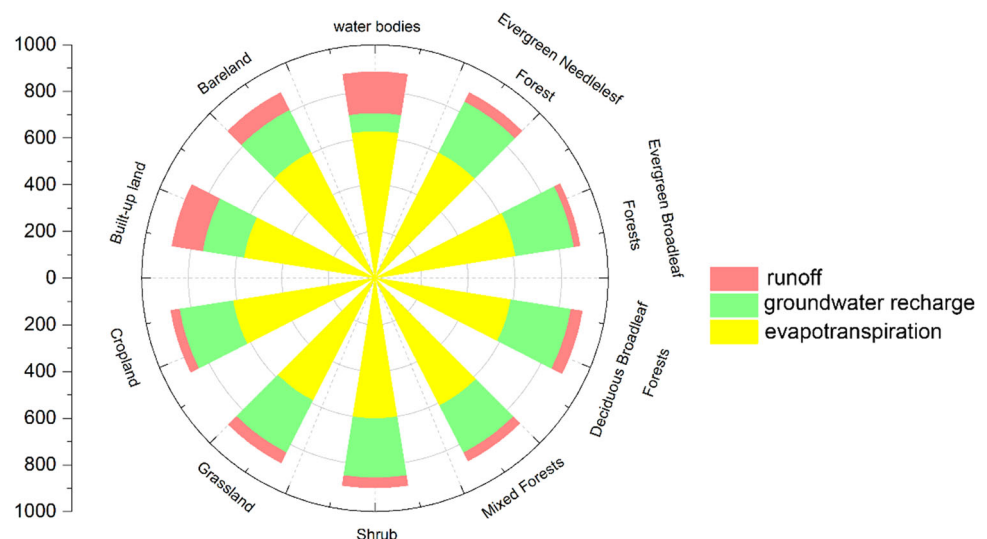
decrease by 11.2% from 1985 to 2008 in the Yangtze River Delta region. Li et al. (2009) presented similar results and pointed out that the combined influences of land use change and climate variability decreased soil water content by 18.8% and 77.1%, total runoff by 9.6% and 95.8%, and evapotranspiration by -8% and 103% , respectively. In general, most findings on the influence of landscape and climate change on the hydrological processes differed greatly depending on natural conditions, such as soil texture and elevation, and the proportion of different landscape types based on the human activities in the study area. Each landscape composition has a potential influence on the state of water bodies, from hydrological pollution to distribution of water balance components (Aguilera et al. 2012; Figuepron et al. 2013). Thus, it will be significant to quantify the water balance components and their dynamics in response to different landscape types, especially in built-up land, which are not sufficiently clear in current studies. Zomlot et al. (2015) indicated that the built-up land had a lower groundwater recharge because of partially impervious surfaces, with average yearly evapotranspiration, groundwater recharge, and surface runoff of 450 mm, 235 mm, and 73 mm, respectively. In the Beiyun River, the findings were somewhat different when equal precipitation was assigned to different landscape types, as shown in Fig. 11. From 2000 to 2012, the greatest change was the conversion of 444 km² of cropland to built-up land. At the same time, the runoff induced by impervious surfaces was three times higher than that by cropland. Water body had the highest runoff and lowest groundwater recharge, influenced by their own water quantity and precipitation (Zomlot et al. 2015). However, although bare land accounted for a lower proportion of the total area, it had nonnegligible runoff higher than that in forest, shrub, grassland, and cropland.

4.2 The effects of landscape indices' variation on discharge at sub-catchment scale

With the effects of urbanization, landscape patterns are altered obviously by the increasing configuration of built-up land (Wu et al. 2011), which can be quantified with different landscape indices, such as edge, shape, aggregation, and diversity aspects (McGarigal et al. 2002). Some studies have examined the relationships between landscape indices and water quality in different cities (Bartsch et al. 2015; Li et al. 2015a). Their results have suggested that many landscape indices have positive or negative effects on water quality, such as NH_3^+ , $-\text{N}$, COD, and heavy metals (Ji et al. 2015), and their findings have indicated that PD, AI, and SPLIT are sensitive to these different water-quality parameters. However, these studies did not focus on change in water quantity based on the influence of landscape pattern variations.

In our study, we explored the correlation between the variations in different landscape indices and discharge at the sub-catchment outlets in the Beiyun River to more fully understand the way in which the landscape pattern changes affect the discharge processes. In the short term (2000–2006), LPI was correlated negatively with discharge, while ED, PD, SPLIT, COHESION, and SHDI were correlated positively, but not significantly, with discharge (Fig. 12). SHDI had the largest correlation coefficient (r) of 0.50, indicating the variation in SHDI had the greatest potential to influence the discharge. With the expansion of urban land, the landscape patterns have changed gradually. As a result, the correlations between selected landscape indices and discharge were higher during the past 13 years than in the first 6 years, suggesting landscape pattern variations are playing an increasing role in the changes in discharge. In contrast, there were negative

Fig. 11 The water balance components in response to different landscape compositions



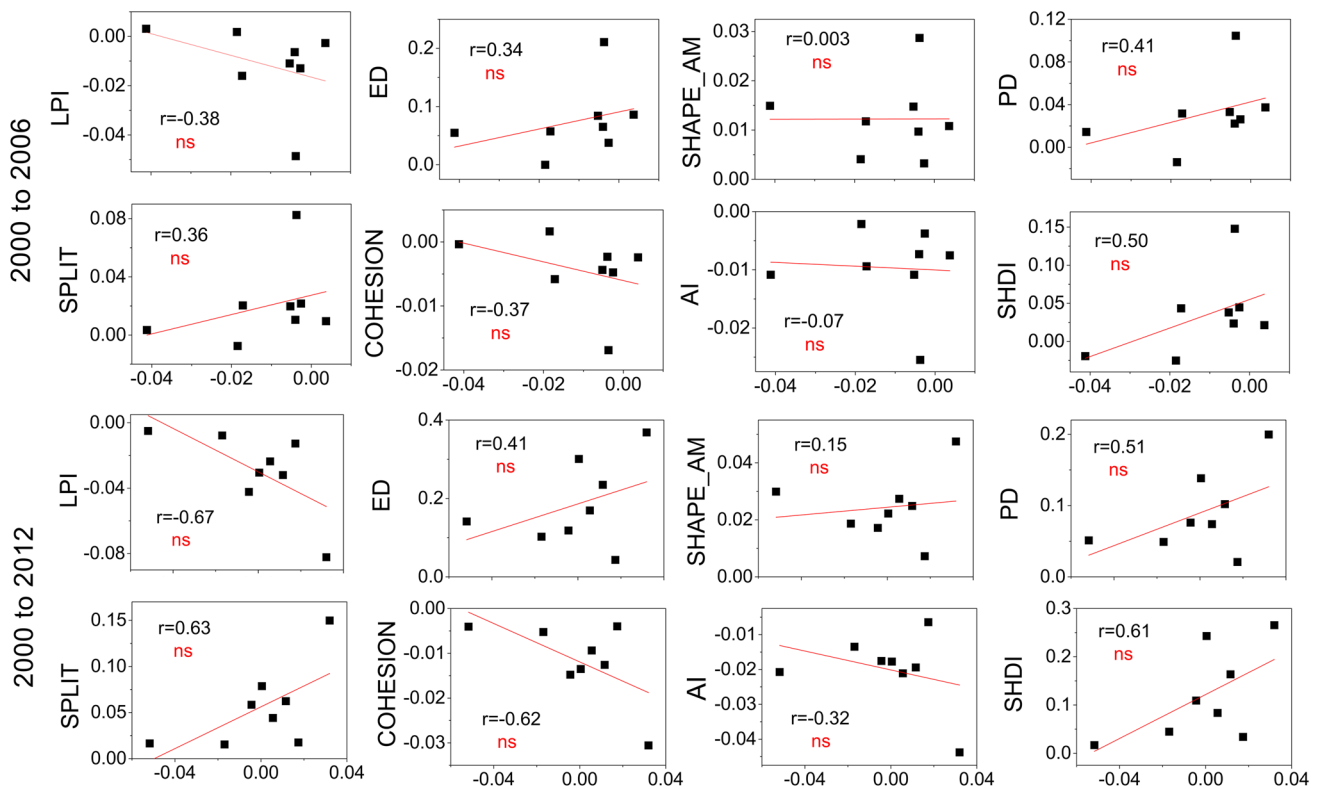


Fig. 12 Correlations between selected landscape index variations and discharge changes during different periods at the sub-catchment scale

correlations between LPI, COHESION, AI, and discharge with correlation coefficients of -0.67 , -0.62 , and -0.32 , respectively, while there was a positive correlation between ED, PD, SPLIT, SHDI, and discharge. On the whole, PD, SPLIT, SHDI, and ED increased slightly, while AI decreased with the increasing discharges from 2000 to 2012. Further, previous studies have shown that scattered patches will lead to lower AI, and higher SPLIT and PD values, and thus change the flow regimes, such as runoff directions and rates, and increase the annual runoff as well (Li et al. 2015b). In addition, Fiener et al. (2011) found disaggregated and splitting patches that may interact depending on their connectivity within different landscapes, which could control water passage from one area to another, including surface runoff (Roberts 2016).

In summary, from 2000 to 2006, the changes in landscape patterns contributed less to the increasing discharge, while the contribution rates increased and were accompanied by higher correlations between landscape index variations and discharge changes on a longer time scale.

4.3 The effect of extreme weather and other factors on flowstream

Although climate change is the primary factor that drives hydrological processes, the responses of water balance

components are not obvious on a short time scale. However, sudden rainstorms bring mountain torrents rushing down, and impose a series of consequences on residents nearby. Therefore, it is important to understand rainstorm distribution, especially storm runoff. During the 17-year study period, two 20-year return rainstorms occurred in July 21, 2012 and June 20, 2016 (Gao 2014; Wang et al. 2017). According to the historical records, during the first rainstorm, the average and maximum levels reached 179.1 mm and 257.0 mm. In response, the maximum discharges of 298 m³/s, 629 m³/s, 478 m³/s, 516 m³/s, and 793 m³/s in this rainstorm, which were ten times higher than their average annual discharge, were distributed in different subcatchments, Wenyuhe, Qinghe, Bahe, Tonghuihe, and Liangshuihe, respectively. In the case of the second rainstorm, the rainfall was heavier, with an average value of 254.3 mm and maximum value of 318 mm, respectively. The tributaries in the Beiyun River took large volumes of discharge, the maximum levels of which were in Qinghe, Bahe, and Tonghuihe, where they reached 284 m³/s, 447 m³/s, and 507 m³/s. It is noteworthy that the Liangshui River downstream of the Beiyun River witnessed the maximum discharge in the entire catchment at 780 m³/s.

Except for landscape composition and climate factors, the sluice gates located in the mainstream and tributaries

(Fig. 2) also play an important role in the control of flow stream (Rady 2016). In the Beiyun River, the main projects for flood control are the Beiguan flood diversion sluice and Yangwa sluice gate. Before the heavy rain, the water levels in front of these sluice gates had been decreased to reduce the peak flow. In July 21, 2012, the water level was dropped to 17.6 m after opening the Beiguan sluice gate, while it was lower than 12 m downstream of the Yangwa sluice gate. As a result, a total capacity of 12 million m³ was reserved to ensure the smooth discharge of flood and reduced discharge pressure further in the Beiyun River. More importantly, the discharge in the mainstream and tributaries received a reasonable allocation through the operation and coordination of sluice gates. Ultimately, it was able to minimize the threat of flood to residents and buildings around Beiyun River. Coping with the heavier rainfall on June 20, 2016, the measure was similar, with a storage capacity of 7 million m³ prepared. Therefore, the actual runoff volume in peak flow was lower than that simulated by the WetSpa extension for the control of sluice gates.

In addition, there are also close relationships between drought and hydrological alterations, which have been explored by many studies (Wan et al. 2018; Veettil et al. 2018).

Generally, extreme climatic events, rainstorm and drought, have occurred more frequently in recent decades, especially in summer, and have had a significant effect on runoff. Because of the coordination among different sluice gates, the peak flows from different tributaries were staggered and the sluice gates caused the discharges to be controlled more artificially.

5 Conclusion

This study presented a case to illustrate the combined and individual effects of landscape composition variations and climate change on hydrological processes in the Beiyun River based on the WetSpa extension model. Our major findings were as follows:

- (1) The encroachment of built-up land on cropland was the main cause of altered landscape compositions, which were characterized by decentralization, fragmentation, and diversity attributable to human activities. Therefore, the expansion of built-up land on cropland should be controlled and the proportions of other landscape types, such as forest and grassland in urban centers of Beiyun river midstream, should be increased reasonably.
- (2) The scenario analysis indicated that combined landscape variation and climate change increased the

total runoff and groundwater storage in the Beiyun River. However, at a short time scale, the individual climate change played a positive effect on increased surface runoff while landscape variation had a negative effect on surface runoff. At a longer time scale, climate change and landscape variation both have positive effects on surface runoff. Therefore, landscape variation caused by human activities have long-term effects on hydrology. Through the ordered human activity interferences, the hydrological elements could be altered in the direction of human expectation.

- (3) It is notable that landscape patterns played a more important role on the increased runoff, in which large patch index, splitting index, and patch cohesion index had higher potentials than other landscape pattern indices. Thus, water resource managers should pay more attentions to landscape planning to control water distribution more effectively.
- (4) Precipitation demonstrated an increasing trend accompanied by several extreme weather events during the period from 2012 to 2016. Specifically, heavy rains altered the hydrological processes greatly and posed potential threats to the environment within a short time. Thus, the analysis of the effect of sluice gates on runoff can help provide a basis for runoff regulation during extreme weather.

Acknowledgements The research was financially supported by the National Natural Sciences Foundation of China (41530635; 41571173) and National Key Research and Development Project (No. 2016YFC0502103).

References

- Aguilera R, Sabater S, Marcé R (2012) In-stream nutrient flux and retention in relation to land use in the Llobregat River Basin. *The Llobregat*, Springer Berlin, Heidelberg, pp 69–92
- Ahiablame L, Sheshukov AY, Rahmani V, Moriasi D (2017) Annual baseflow variations as influenced by climate variability and agricultural land use change in the Missouri River Basin. *J Hydrol* 551:188–202
- Allen RG (2000) Using the FAO-56 dual crop coefficient method over an irrigated region as part of an evapotranspiration intercomparison study. *J Hydrol* 229:27–41
- Allen RG, Pereira LS, Raes D, Smith M (1998) Crop evapotranspiration—guidelines for computing crop water requirements FAO irrigation and drainage paper 56. FAO, Roma
- Andréassian V (2004) Waters and forests: from historical controversy to scientific debate. *J Hydrol* 291:1–27
- Bartsch WM, Axler RP, Host GE (2015) Evaluating a Great Lakes scale landscape stressor index to assess water quality in the St. Louis River Area of Concern. *J Great Lakes Res* 41(1):99–110
- Brown AE, Zhang L, McMahon TA, Western AW, Vertessy RA (2005) A review of paired catchment studies for determining

- changes in water yield resulting from alterations in vegetation. *J Hydrol* 310:28–61
- Chen Y, Pang S, Geng R, Wang X, Bao L (2015) Fluxes of the main contaminant in Beiyun River. *Acta Sci Circum* 35:2167–2176
- Chen J, Theller L, Gitau MW, Engel BA, Harbor JM (2017) Urbanization impacts on surface runoff of the contiguous United States. *J Environ Manag* 187:470–481
- Cuo L, Beyene TK, Voisin N, Su F, Lettenmaier DP, Alberti M, Richey JE (2011) Effects of mid-twenty-first century climate and land cover change on the hydrology of the Puget Sound basin, Washington. *Hydrol Process* 25:1729–1753
- Eum HI, Dibike Y, Prowse T (2016) Comparative evaluation of the effects of climate and land-cover changes on hydrologic responses of the Muskeg River, Alberta, Canada. *J Hydrol Reg Stud* 8:198–221
- Fan M, Shibata H (2015) Simulation of watershed hydrology and stream water quality under land use and climate change scenarios in Teshio River watershed, northern Japan. *Ecol Indic* 50:79–89
- Fienier P, Auerswald K, Oost KV (2011) Spatio-temporal patterns in land use and management affecting surface runoff response of agricultural catchments—A review. *Earth Sci Rev* 106(1):92–104
- Fiquepron JS, Garcia S, Stenger A (2013) Land use impact on water quality: valuing forest services in terms of the water supply sector. *J Environ Manage* 126:113–121
- Gao Y (2014) Analysis of Beiyunhe River heavy rain flood in 2012. *Water Sci Eng Technol* 5:41–43
- Gao YL, Tang JK, Qian J et al (2010) The effects of land use and land cover on water environment: a review. *Yellow River* 32(12):16–18
- Han J, Meng X, Zhou X, Yi B, Liu M, Xiang W (2017) A long-term analysis of urbanization process, landscape change, and carbon sources and sinks: a case study in China's Yangtze River Delta region. *J Clean Prod* 141:1040–1050
- Jeppesen E, Kronvang B, Meerhoff M, Søndergaard M, Hansen K (2016) Climate change effects on runoff, catchment phosphorus loading and lake ecological state, and potential adaptations. *J Environ Qual* 38:1930–1941
- Ji L, Fu C, Yang B, Liu Y (2013) Analysis of “7. 21” rainstorm flood dispatching in Beiyun River. *Beijing Water Aff* 1:9–11
- Ji DQ, Wen Y, Wei JB, Wu ZF, Liu Q, Cheng J (2015) Relationships between landscape spatial characteristics and surface water quality in the Liu Xi River watershed. *Acta Ecol Sinica* 35(2):246–253
- Kim S, Kim BS, Jun H, Kim HS (2014) Assessment of future water resources and water scarcity considering the factors of climate change and social–environmental change in Han River basin, Korea. *Stoch Environ Res Risk Assess* 28:1999–2014
- Kundu S, Khare D, Mondal A (2017) Individual and combined impacts of future climate and land use changes on the water balance. *Ecol Eng* 105:42–57
- Li Z, Liu W-z, Zhang X-c, Zheng F-l (2009) Impacts of land use change and climate variability on hydrology in an agricultural catchment on the Loess Plateau of China. *J Hydrol* 377(1–2):35–42
- Li G, Xiang X, Tong Y (2013) Impact assessment of urbanization on flood risk in the Yangtze River Delta. *Stoch Environ Res Risk Assess* 27:1683–1693
- Li Y, Li Y, Qureshi S, Kappas M, Hubacek K (2015a) On the relationship between landscape ecological patterns and water quality across gradient zones of rapid urbanization in coastal China. *Ecol Model* 318:100–108
- Li B, Zhou W, Zhao Y, Ju Q, Yu Z, Liang Z, Acharya K (2015b) Using the SPEI to assess recent climate change in the Yarlung Zangbo River Basin, South Tibet. *Water* 7(10):5474–5486
- Li S, Xiong L, Li HY (2016) Attributing runoff changes to climate variability and human activities: uncertainty analysis using four monthly water balance models. *Stoch Environ Res Risk Assess* 30:251–269
- Liu J, Shi Z (2017) Quantifying land-use change impacts on the dynamic evolution of flood vulnerability. *Land Use Policy* 65:198–210
- Liu Y, Smedt F (2004) WetSpa extension, a GIS-based hydrologic model for flood prediction and watershed management. *User Manual* 388:279–360
- Liu YB, Gebremeskel S, Smedt FD, Hoffmann L, Pfister L (2003) A diffusive transport approach for flow routing in GIS-based flood modeling. *J Hydrol* 283:91–106
- Liu S et al (2017) Ecosystem services and landscape change associated with plantation expansion in a tropical rainforest region of Southwest China. *Ecol Model* 353:129–138
- Locatelli L, Mark O, Mikkelsen PS, Nielsen KA, Deletic A, Roldin M, Binning PJ (2017) Hydrologic impact of urbanization with extensive stormwater infiltration. *J Hydrol* 544:524–537
- McGarigal K, Cushman S, Neel MC, Ene E (2002) FRAGSTATS: spatial pattern analysis program for categorical maps. University of Massachusetts, Boston
- Miller JD, Kim H, Kjeldsen TR, et al (2014) Assessing the impact of urbanization on storm runoff in a peri-urban catchment using historical change in impervious cover. *J Hydrol* 515:59–70
- Mwangi HM, Julich S, Patil SD, McDonald MA, Feger K-H (2016) Relative contribution of land use change and climate variability on discharge of upper Mara River, Kenya. *J Hydrol Reg Stud* 5:244–260
- Napoli M, Massetti L, Orlandini S (2017) Hydrological response to land use and climate changes in a rural hilly basin in Italy. *CATENA* 157:1–11
- Nash JE, Sutcliffe JV (1970) River flow forecasting through conceptual models. *J Hydrol* 10:282–290
- NOAA (2016) Global climate change indicators. NOAA-National Centers for Environmental Information, Asheville
- Nourani V, Saeidifarzad B (2017) Detection of land use/cover change effect on watershed's response in generating runoff using computational intelligence approaches. *Stoch Environ Res Risk Assess* 1:1–17
- Ouyang W, Wang W, Hao F, Song K, Wang Y (2010) Pollution characterization of urban stormwater runoff on different underlying surface conditions. *China Environ Sci* 30:1249–1256
- Putro B, Kjeldsen TR, Hutchins MG, Miller J (2016) An empirical investigation of climate and land-use effects on water quantity and quality in two urbanising catchments in the southern United Kingdom. *Sci Total Environ* 548–549:164–172
- Qi X, Liu H, Han H, Chai W, Qu J (2013) A study of metal contamination in sediments in Beisan River System. *Acta Sci Circum* 33:117–124
- Rady RAE-H (2016) Modeling of flow characteristics beneath vertical and inclined sluice gates using artificial neural networks. *Ain Shams Eng J* 7:917–924
- Roberts AD (2016) The effects of current landscape configuration on streamflow within selected small watersheds of the Atlanta metropolitan region. *J Hydrol Regional Studies* 5:276–292
- Schütte S, Schulze RE (2017) Projected impacts of urbanisation on hydrological resource flows: a case study within the uMngeni Catchment, South Africa. *J Environ Manag* 196:527–543
- Shan B, Guan Y, Zhang H (2011) Analysis of the heavy metal pollution features and the assessment situation in the lower reach of the North Canal. *J Saf Environ* 11:141–145
- Sofia G, Roder G, Fontana GD, Tarolli P (2017) Flood dynamics in urbanised landscapes: 100 years of climate and humans' interaction. *Sci Rep* 7:40527. <https://doi.org/10.1038/srep40527>

- Su S, Xiao R, Jiang Z, Zhang Y (2012) Characterizing landscape pattern and ecosystem service value changes for urbanization impacts at an eco-regional scale. *Appl Geogr* 34:295–305
- Su S, Ma X, Xiao R (2014) Agricultural landscape pattern changes in response to urbanization at ecoregional scale. *Ecol Ind* 40:10–18
- Tomer MD, Schilling KE (2009) A simple approach to distinguish land-use and climate-change effects on watershed hydrology. *J Hydrol* 376:24–33
- Veettil VA, Konapala G, Mishra AK, Li HY (2018) Sensitivity of drought resilience–vulnerability–exposure to hydrologic ratios in contiguous United States. *J Hydrol* 564:294–306
- Verbeiren B, Voorde TVD, Canters F, Binard M, Cornet Y, Batelaan O (2013) Assessing urbanisation effects on rainfall–runoff using a remote sensing supported modelling strategy. *Int J Appl Earth Obs Geoinf* 21:92–102
- Wan WH, Zhao JS, Li HY, Mishra A, Hejazi M, Lu H, Demissie Y, Wang H (2018) A holistic view of water management impacts on future droughts: a global multimodel analysis. *J Geophys Res Atmos* 123(11):5947–5972
- Wang Z, Batelaan O, Smedt FD (1996) A distributed model for water and energy transfer between soil, plants and atmosphere (WetSpa). *Phys Chem Earth* 21:189–193
- Wang C, Fu C, Ji L, Liu Y, Liu Z (2017) Analysis of “7. 20” rainstorm flood dispatching in Beiyun River. *Beijing Water Aff* 1:39–42
- Wu JG, Darrel G, Alexander J, Buyantuyev A, Redman CL (2011) Quantifying spatiotemporal patterns of urbanization: the case of the two fastest growing metropolitan regions in the United States. *Ecol Complex* 8(1):1–8
- Xian W, Shao H, Zhou W (2005) Process of land use/land cover change in the area of middle and lower reach of Jialingjiang River. *Prog Geogr* 24:114–121
- Xiao R, Ouyang Z, Li W, Zhang Z, Gregory TJ (2005) A review of the eco-environmental consequences of urban heat islands. *Acta Ecol Sin* 25:2055–2060
- Xiao R, Su S, Zhang Z, Qi J, Jiang D, Wu J (2013) Dynamics of soil sealing and soil landscape patterns under rapid urbanization. *CATENA* 109:1–12
- Yang C, Yang Z, Nie Y, He X, Hu C (2012a) Adsorption of heavy metals Cu, Pb, Zn over top sediment in North River Canal Chinese. *J Environ Eng* 6:3438–3442
- Yang Z, Nie Y, Hu C (2012b) Migration and transformation of heavy metals at solid/water interface in Beiyunhe River. *Chin J Environ Eng* 6:3455–3465
- Yao L, Wei W, Chen L (2006) How does imperviousness impact the urban rainfall–runoff process under various storm cases? *Ecol Ind* 60:893–905
- Yuan S, Zhang W, Zhang B (2014) Heavy metal contaminant distribution features and the diffusion flux estimation in the sediments of Shahe reservoir, Beijing. *J Saf Environ* 14:245–249
- Zhang Q, Sun P, Jiang T, Tu X, Chen X (2011) Spatio-temporal patterns of hydrological processes and their responses to human activities in the Poyang Lake basin, China. *Hydrol Sci J* 56:305–318
- Zhang A, Zhang C, Fu G, Wang B, Bao Z, Zheng H (2012) Assessments of impacts of climate change and human activities on runoff with SWAT for the Huifa River Basin, Northeast China. *Water Resour Manag* 26:2199–2217
- Zhang Q, Gu X, Singh VP, Chen X (2015) Evaluation of ecological instream flow using multiple ecological indicators with consideration of hydrological alterations. *J Hydrol* 529:711–722
- Zhang Q, Liu J, Singh VP, Gu X, Chen X (2016) Evaluation of impacts of climate change and human activities on streamflow in the Poyang Lake basin, China. *Hydrol Process* 30:2562–2576
- Zhang Y, Liu S, Cheng F et al (2017) WetSpa-based study of the effects of urbanization on the water balance components at regional and quadrat scales in Beijing, China. *Water* 10(1):5
- Zhao Q, Liu S, Deng L, Dong S, Wang C, Yang Z, Yang J (2012) Landscape change and hydrologic alteration associated with dam construction. *Int J Appl Earth Obs Geoinf* 16:17–26
- Zhou F, Xu Y, Chen Y, Xu C-Y, Gao Y, Du J (2013) Hydrological response to urbanization at different spatio-temporal scales simulated by coupling of CLUE-S and the SWAT model in the Yangtze River Delta region. *J Hydrol* 485:113–125
- Zhou J, He D, Xie Y (2015) Integrated SWAT model and statistical downscaling for estimating streamflow response to climate change in the Lake Dianchi watershed, China. *Stoch Environ Res Risk Assess* 29:1193–1210
- Zomlot Z, Verbeiren B, Huysmans M, Batelaan O (2015) Spatial distribution of groundwater recharge and base flow: assessment of controlling factors. *J Hydrol Reg Stud* 4:349–368